

Additional Materials

1.1 Comparisons to Other Operators

We show that several other proposed operators for quadrilateral meshes can be realized by our operations under common situations.

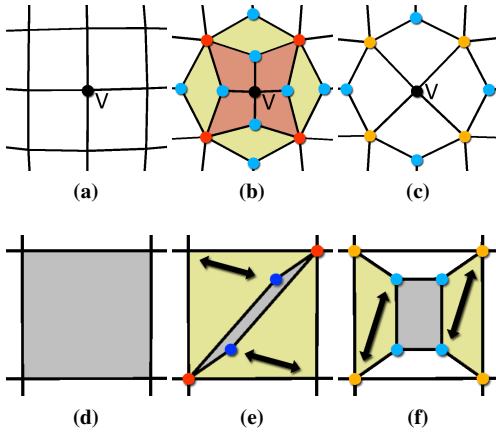


Figure 2: Realization of vertex rotation and quadrilateral flip $(2,0) - (0,2)$ (extrusion) by our operations. (a) Before we perform vertex rotation around v . (b) First we perform edge splits around the closest loop around v (quads created are shown in yellow), then we collapse quads adjacent to v (red). (c) Final result. (d) Before we perform extrusion in the face. (e) First we perform two edge splits along two pairs of consecutive sides, creating two temporary v_2 vertices. (f) We perform two more edge splits. The result is an extruded face within the original face.

We first discuss the comprehensive collection of local editing operators proposed in [Tarini et al. 2010]. **Edge rotate** is exactly edge flip. **Vertex rotate** is equivalent to a combination of quad collapses and edge splits, as shown in Figure 2. **Diagonal collapse** is exactly quad collapse. **Edge collapse**, as stated in the paper, is equivalent to one vertex rotation followed by one diagonal collapse, thus is equivalent to a combination of our operations. **Doublet removal** and **singlet removal** are special cases of quad collapse.

The **quadrilateral flips** proposed in [Bern and Eppstein 2001], which correspond to swapping the top and bottom views of a cube, can be realized by our operators. In particular in Figure 2 we show the equivalent sequence of edge splits for the $(2,0) - (0,2)$ case which resembles the extrusion operation commonly found in 3D sculpting tools.

GP operators [Bommes et al. 2011], of which **poly-chord collapse** [Daniels et al. 2008] is a special case, can also be realized by our operations when applied to a convex region with a single boundary, as shown in Figure 3. A key requirement for the GP operators is that they must circulate a loop with total turning angles of 0 because there must be the same numbers of right turns and left turns in the state machine. In other words the convex region is cut into two parts, one within the loop and one adjacent to the boundary. By Equation 1 we know that the total valence deficiency within the loop is 4, e.g. $4 \sqrt{3}$ vertices. Thus one strategy to realize GP operators by our four operations is to move the irregular vertices within the region enclosed by the loop to achieve the same topology effects. However, this strategy does not work for all quad meshes, e.g., for a genus one mesh (torus) we cannot find such convex region (the connected part surrounding the loop always has two boundaries). Finding a mapping between pair-wise movements and

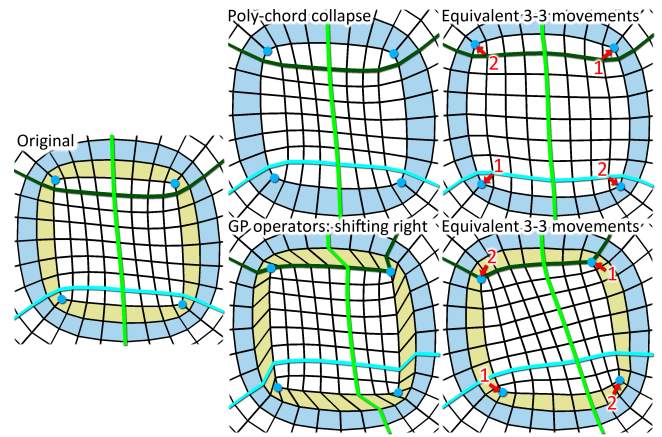


Figure 3: Realization of poly-chord collapse and GP operators (shifting right) by our operations. (left) Original mesh. The loop of quads to be collapsed or shifted are denoted in yellow. Blue faces and colored paths are marked to assist comparisons. (top row) Poly-chord collapse (left) is equivalent to a series of 3-3 pair movements (right). Red arrows (numbered by orders) denote the directions of movements. (bottom row) Shifting right by GP operators (left) is equivalent to a series of 3-3 pair movements (right).

GP operators in the general case is an interesting topic for future research.

1.2 Proof of Lemma 7.8

Proof We first make the following comment. A region R is convex if and only if for any vertices $u, v \in R$ any shortest path connecting them is also in R . A sketch of the proof is as follows. Assume that the region is convex yet there exist $u, v \in R$ such that a shortest path γ connecting u and v is partially outside R . Then γ must intersect ∂R an even number of times. Consider the first two such intersection points w_1 and w_2 . Then there must be a negative angle of turn on ∂R between w_1 and w_2 . This contradicts that R is convex. For the other direction of the comment, assume that R is not convex yet for any $u, v \in R$ we have $\gamma \subset R$ where γ is any shortest path connecting u and v . In this case we can find two sides of ∂R that have a negative turn since R is concave. Let the two sides be s_i and s_{i+1} and the point of turn is w . Consider the vertices on ∂R immediately before and after w . They are located on s_i and s_{i+1} , respectively. Between these vertices there is a shortest path connecting them but is outside R , again a contradiction.

Given the comment, it is straightforward to show that R_α is unique. Assume there are two such minimal regions $U \neq V$. Then $W = U \cap V$ must be strictly smaller than U or V . Say W is strictly smaller than U . Furthermore, since U and V are convex they both satisfy the condition that for any vertices $u, v \in R$ any shortest path connecting them is also in R . Consequently, W satisfies this condition as well yet it is smaller than U . Thus U is not minimal which is a contradiction.

By Equation 1 it is easy to show that every convex region in a regular mesh must form a rectangular grid of size d_1 by d_2 . Consequently R_α has to be a rectangular grid because it does not include irregular interior vertices. Furthermore, v_1 and v_2 need to be located at the opposing corners otherwise the rectangular grid is not minimal. Because all vertices other than v_1 and v_2 are regular, two adjacent sides of R_α become v_1 and v_2 's connecting separatrices of length d_1 and d_2 . All possible configurations of R_α are shown in Figure 13b. ■

1.3 Proof for Theorem 7.1

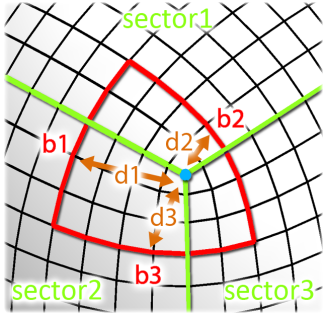


Figure 4: A v_3 vertex in blue and the three separatrices in green. The separatrices divide the neighborhood of the irregular vertex into three sectors. Each boundary segment (red) intersects exactly two sectors, and is distance increasing in one sector and distance decreasing in the other.

Definition 1.1 Given a mesh M and an irregular vertex v_0 with a valence of $l(v_0)$, a valid neighborhood R of v_0 is a non-degenerate region in M whose boundary is a regular loop and whose only irregular vertex is v_0 .

The separatrices of v_0 divide any of its valid neighborhood into $l(v_0)$ sectors, with each sector bounded by two separatrices and ∂R . A straight path inside a valid neighborhood R can intersect exactly two sectors, resulting in two *pure segments*, i.e., a segment contained entirely inside one sector. Along each segment the graph distance of the vertices on the segment to the irregular vertex v_0 will monotonically increase or decrease along the segment (see Figure 4). One of the two segments must be distance increasing while the other is a distance decreasing. The length of the straight path is the number of edges on the path, and the distance of the path to the irregular singularity v_0 is the minimal graph distance of any vertex on the segment to v_0 .

The following lemmas are needed to prove Theorem 7.1.

Lemma 1.2 Consider a convex region R that contains only one irregular vertex v_0 in its interior. The boundary of R must contain $l(v_0)$ turns, each of which with an angle of turn of $\frac{\pi}{2}$.

Proof Since R is simply connected and there is only one irregular vertex inside R , from Equation 1 we have $\sum_{v \in \partial R} (m(v) - 2) = l(v_0)$. Given that R is convex, for any turn point on ∂R we have $m(v) = 3$. Consequently, there can be exactly $l(v_0)$ turns along ∂R . ■

Lemma 1.3 Consider a convex region R that contains only one irregular vertex v_0 in its interior. Let b_i be the length of segment s_i and d_i the graph distance of s_i to v_0 . Then we have $b_i = d_{i-1} + d_{i+1}$.

Proof From previous discussion we know that each boundary segment intersects two sectors, and each sector intersects two sides of ∂R . Let $q_{i,j} = s_i \cap S_j$ where S_j is the j -th sector. Assume $q_{i,j} \neq \emptyset$ if and only if $j = i$ or $j = i + 1$. Since S_j intersects s_{j-1} and s_j , we have $\text{length}(q_{i,j}) = d_{i-1}$ and $\text{length}(q_{i-1,j}) = d_i$ (see diagram). Consequently, $b_i = \text{length}(q_{i,j}) + \text{length}(q_{i,j+1}) = d_{i-1} + d_{i+1}$. ■

We now present the proof for Theorem 7.1.

Proof Given Lemmas 1.2 and 1.3, we know a convex region R satisfying the condition of this theorem will have $l(v_0)$ sides and the length and distance of these sides satisfy

$$b_i = d_{i-1} + d_{i+1} \quad (4)$$

for all $0 \leq i < l(v_0)$. Assume that we have requadrangled the interior of region R such that there is a unique irregular vertex v'_0 . Let d'_i be distance of v'_0 to side s_i . Then we have

$$b_i = d'_{i-1} + d'_{i+1} \quad (5)$$

In other words, the configurations of the interior of R before and after the requadrangulation satisfy the same system of equations $Ad = b$ where $d = [d_1, \dots, d_{l(v_0)}]$, $b = [b_1, \dots, b_{l(v_0)}]$, and $A = (a_{ij})$ in which $a_{ij} = 0$ except $a_{i,i+1} = a_{i+1,i} = 1$. Notice that A has a non-zero determinant when $l(v_0) \bmod 4 \neq 0$, which means there is a unique solution for d_i . Consequently, the requadrangulations before and after represent the same configuration and the irregular vertex cannot be moved. If the valence is a multiple of four the determinant of A is 0 and multiple solutions exist. ■

In fact, the requirement in the theorem that the enclosing polygon is convex can be relaxed. Basically, if the polygon can be enlarged to a convex one without including any additional irregular vertex, then it is impossible to move the irregular vertex in the original polygon which may be concave. While this theorem only states that moving a single irregular vertex within a convex region is impossible, we have not found a case where we can move an irregular vertex in practice.

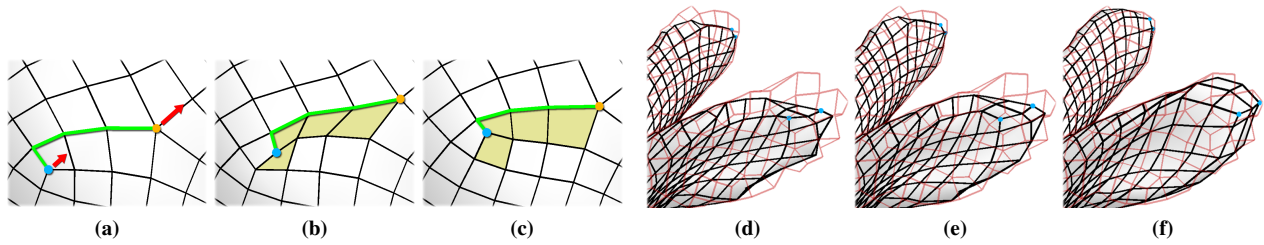


Figure 5: Laplacian smoothing and pulling schemes. (a) to (c) Apply Laplacian smoothing to improve the positions of vertices adjacent to a 3 – 5 pair movement. (d) to (f) An area with a large difference to the original mesh (red) is pulled iteratively to the original mesh.

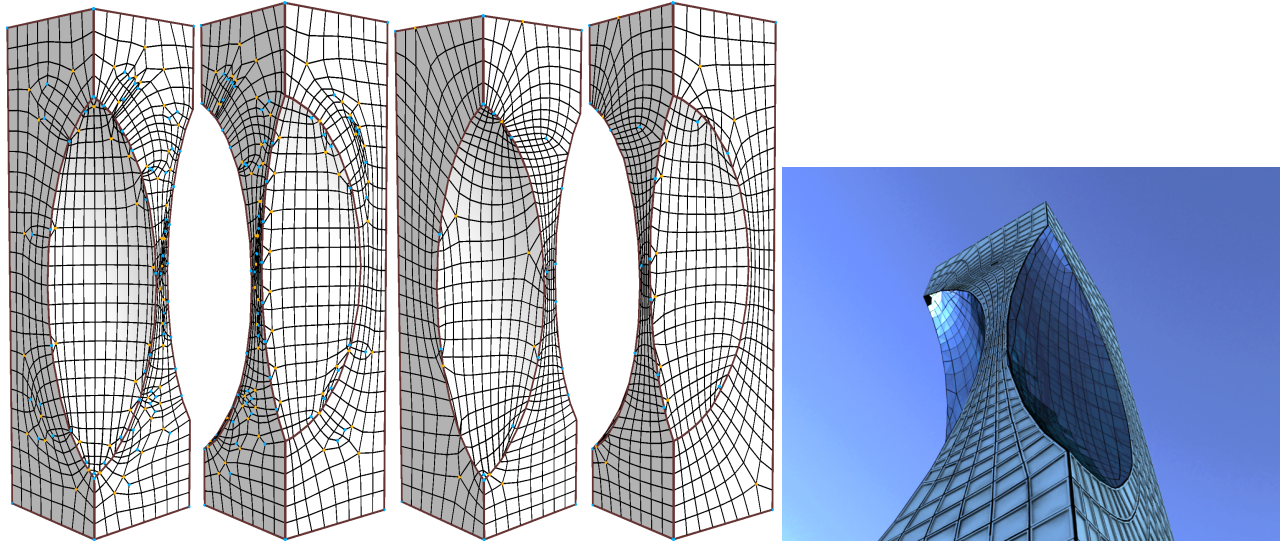


Figure 6: From left to right: the first two images show two views of a tower model with a large number of irregular vertices and small mesh faces due to the intersection computation in a professional modeling package. The second two views show how we reduced several singularities and improved the mesh layout. The last image is a rendered model. This example is a motivation for future work where we would like to investigate editing operations to control mesh lines.

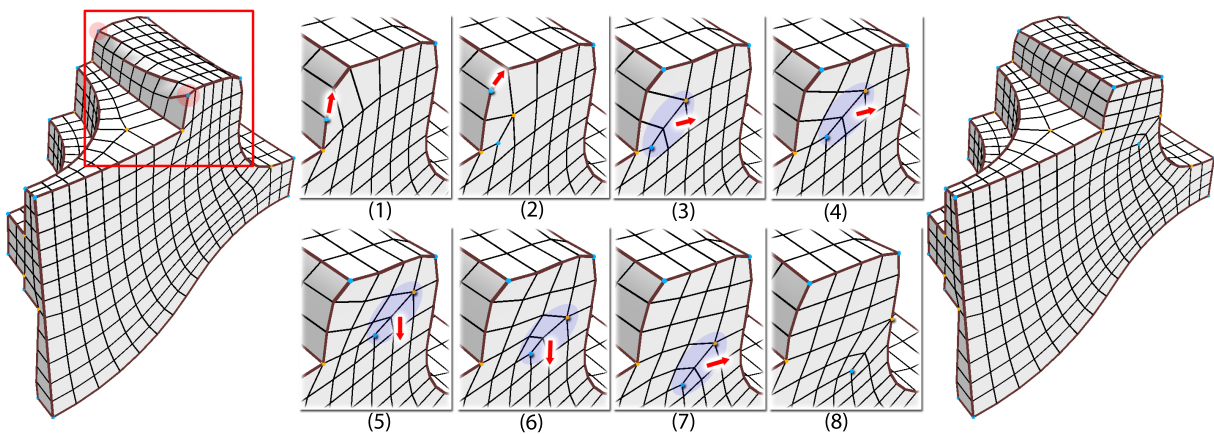


Figure 7: Using our editing framework to improve a remeshed fan disk model from Mixed-Integer Quadrangulation [Bommes et al. 2009]. (left) Original mesh with an ill-shaped upper part. The mis-aligned v_3 vertex pair distort the structure. (1) Geometry improved by adjusting the positions of adjacent vertices. However, bad shaped faces emerge because the local connectivity does not match the desired shape. (2) to (3) The misplaced v_3 vertex is moved to its proper location by an edge flip. (4) to (8) the created 3 – 5 pair is moved to its proper location. (right) Mesh improved by our editing framework. The upper part now has a nice structure with aligned irregular vertices and consistent face strips.

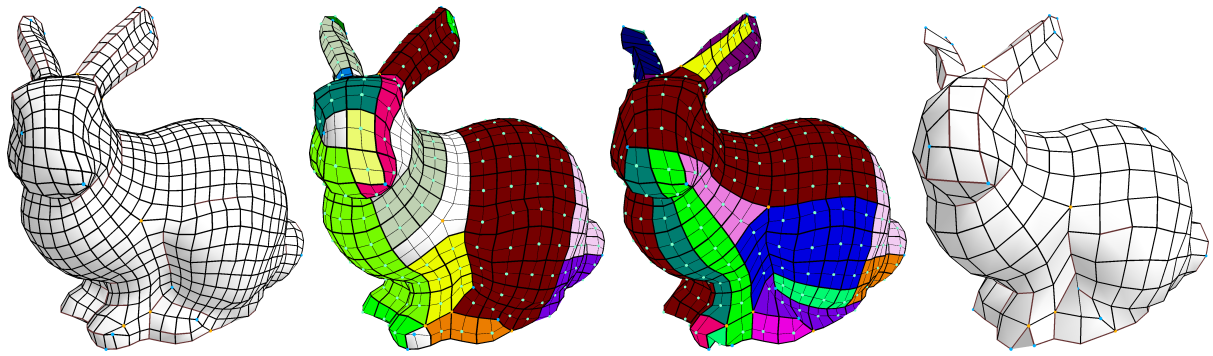


Figure 8: *Editing a mesh to align separatrices.*